

Research Article

Image Theory for Neumann Functions in the Prolate Spheroidal Geometry

Changfeng Xue,¹ Robert Edmiston,² and Shaozhong Deng ²

¹School of Mathematics and Physics, Yancheng Institute of Technology, Yancheng, Jiangsu 224051, China

²Department of Mathematics and Statistics, University of North Carolina at Charlotte, Charlotte, NC 28223, USA

Correspondence should be addressed to Shaozhong Deng; shaodeng@uncc.edu

Received 19 September 2017; Accepted 4 February 2018; Published 11 March 2018

Academic Editor: Pavel Kurasov

Copyright © 2018 Changfeng Xue et al. This is an open access article distributed under the Creative Commons Attribution License, which permits unrestricted use, distribution, and reproduction in any medium, provided the original work is properly cited.

Interior and exterior Neumann functions for the Laplace operator are derived in terms of prolate spheroidal harmonics with the homogeneous, constant, and nonconstant inhomogeneous boundary conditions. For the interior Neumann functions, an image system is developed to consist of a point image, a line image extending from the point image to infinity along the radial coordinate curve, and a symmetric surface image on the confocal prolate spheroid that passes through the point image. On the other hand, for the exterior Neumann functions, an image system is developed to consist of a point image, a focal line image of uniform density, another line image extending from the point image to the focal line along the radial coordinate curve, and also a symmetric surface image on the confocal prolate spheroid that passes through the point image.

1. Introduction

Let S be a smooth closed surface in \mathbb{R}^3 , with Ω being its interior and Ω^c its exterior, respectively. An interior Neumann function for the Laplace operator is the solution of the following boundary value problem for the potential $N^i(\mathbf{r}, \mathbf{r}_s)$:

$$\Delta N^i(\mathbf{r}, \mathbf{r}_s) = \delta(\mathbf{r} - \mathbf{r}_s), \quad \mathbf{r} \in \Omega, \quad (1a)$$

$$\frac{\partial}{\partial n} N^i(\mathbf{r}, \mathbf{r}_s) = g_S(\mathbf{r}), \quad \mathbf{r} \in S, \quad (1b)$$

where Δ is the Laplace operator, \mathbf{r}_s is a fixed point in the open domain Ω , $\delta(\mathbf{r})$ is the Dirac delta function, $\partial/\partial n$ is the outward normal derivative on the surface S , and $g_S(\mathbf{r})$ is a given function specified on the surface S satisfying the constraint

$$\oint_S g_S(\mathbf{r}) ds = 1. \quad (2)$$

This constraint follows by applying the divergence theorem to (1a). If we further demand the normal derivative to be constant on S , then we arrive at probably the most common

boundary condition used in developing a Neumann-Green's function [1]:

$$\frac{\partial}{\partial n} N^i(\mathbf{r}, \mathbf{r}_s) \equiv \frac{1}{|S|}, \quad \mathbf{r} \in S, \quad (3)$$

where $|S|$ stands for the total surface area of S .

The solutions of a Neumann problem

$$\Delta u(\mathbf{r}) = f(\mathbf{r}), \quad \mathbf{r} \in \Omega, \quad (4a)$$

$$\frac{\partial}{\partial n} u(\mathbf{r}) = \psi(\mathbf{r}), \quad \mathbf{r} \in S, \quad (4b)$$

when they exist, have the following integral representation (see [2], p.286-287):

$$u(\mathbf{r}) = \langle u \rangle + \int_{\Omega} N^i(\mathbf{r}, \mathbf{r}') f(\mathbf{r}') d\mathbf{r}' - \oint_S N^i(\mathbf{r}, \mathbf{r}') \psi(\mathbf{r}') ds', \quad (5)$$

where $\langle u \rangle$ stands for the *weighted* mean value of the solution u on S ; namely, $\langle u \rangle = \oint_S g_S(\mathbf{r}) u(\mathbf{r}) ds$, which can be chosen to

be zero to simplify the equation. All other solutions to (4a) and (4b) can be obtained by adding an arbitrary constant to this solution.

Likely, an exterior Neumann function for the Laplace operator is the solution of the following boundary value problem for the potential $N^e(\mathbf{r}, \mathbf{r}_s)$:

$$\Delta N^e(\mathbf{r}, \mathbf{r}_s) = \delta(\mathbf{r} - \mathbf{r}_s), \quad \mathbf{r} \in \Omega^c, \quad (6a)$$

$$\frac{\partial}{\partial n} N^e(\mathbf{r}, \mathbf{r}_s) = -g_s(\mathbf{r}), \quad \mathbf{r} \in S, \quad (6b)$$

$$N^e(\mathbf{r}, \mathbf{r}_s) = O(1/|\mathbf{r}|^2), \quad |\mathbf{r}| \rightarrow +\infty, \quad (6c)$$

where \mathbf{r}_s now is a given point in the open domain Ω^c .

Neumann functions are analogous to Green's functions for Dirichlet problems, so they are often also called Green's function for the Neumann problem or Green's function of the second kind. While Dirichlet-Green's functions are generally used for electrostatic problems where the potential is specified on bounding surfaces, Neumann-Green's functions are often useful for finding temperature distributions where the bounding surfaces have specified currents. Similar to Dirichlet-Green's functions, a Neumann-Green function can also be decomposed into a singular and a regular part as [2]

$$N(\mathbf{r}, \mathbf{r}_s) = -\frac{1}{4\pi|\mathbf{r} - \mathbf{r}_s|} + R(\mathbf{r}, \mathbf{r}_s), \quad (7)$$

where $R(\mathbf{r}, \mathbf{r}_s)$ is a harmonic function that secures the satisfaction of the boundary conditions. In what follows, $R(\mathbf{r}, \mathbf{r}_s)$ is also called the reflected part of the Neumann function.

An image system for a Neumann function is a system of fictitious sources inside the complement of the fundamental domain that produces a potential equal to the reflected part of the Neumann function. These fictitious sources are commonly called images because they are located not in the real domain of interest for the problem but in its complement. In general, such an image system is not unique. There are all types of images, from isolated point images to continuous distributions of images on lines, curves, and surfaces to combinations of these images. While image theories for Dirichlet-Green's functions have been studied quite extensively in the literature [3–11], much less work has been done with image theories for Neumann-Green's functions.

In their interesting article [12], Dassios and Sten studied the Neumann function with the constant boundary condition and the corresponding image system in spherical and ellipsoidal geometry. For example, they have found that, in the spherical case, an image system for the exterior spherical Neumann function may consist of (i) a point image at the origin with strength -1 , (ii) a point image at the conventional Kelvin image point $\mathbf{r}_k = (a/r_s)^2 \mathbf{r}_s$ with strength a/r_s , where a is the radius of the sphere, and (iii) a uniform line image with strength $-1/a$ on the line segment between the origin and the Kelvin image point \mathbf{r}_k . On the other hand, an image system for the interior spherical Neumann function may consist of (i) a

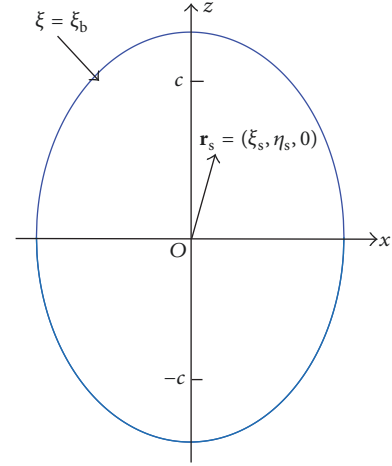


FIGURE 1: A prolate spheroid is centered at the origin, its focal axis is aligned with the z -axis, and its interfocal distance is $2c$. In terms of the prolate spheroidal coordinates (ξ, η, ϕ) defined in the main text, the prolate spheroid is determined by $\xi = \xi_b$. A unit source is located at $\mathbf{r}_s = (\xi_s, \eta_s, 0)$ inside the spheroid.

point image at \mathbf{r}_k with strength a/r_s and (ii) a line image that extends from \mathbf{r}_k radially to infinity with field-point dependent charge density.

In the present work, we shall study Neumann functions and their image systems for the Laplace operator in the prolate spheroidal geometry. Although in theory the case to be considered here is a special case of that studied in [12], the authors still believe it is much beneficial to study it separately because the Neumann functions and their image systems in the ellipsoidal geometry have to be constructed using ellipsoidal harmonics, while those in the prolate spheroidal geometry can be constructed using prolate spheroidal harmonics, but the ellipsoidal harmonics are much more complicated to handle than the spheroidal ones. In addition, it seems that [12] contains several mistakes of omission and commission [13]. The present paper is organized as follows. Section 2 provides a brief introduction to the prolate spheroidal coordinates and to the prolate spheroidal harmonics. Then, interior and exterior Neumann functions and their image systems for the Laplace operator in the prolate spheroidal geometry are developed in Sections 3 and 4, respectively. Finally, some concluding remarks are given in Section 5.

2. Elements of Prolate Spheroidal Harmonics

Prolate spheroid S is defined by

$$\frac{x^2 + y^2}{a^2} + \frac{z^2}{b^2} = 1, \quad (8)$$

where $b > a > 0$. Here, the focal symmetry axis of the spheroid is aligned with the z -axis, and the interfocal distance is $2c$ with $c = \sqrt{b^2 - a^2}$; see Figure 1.

In this paper, the prolate spheroidal coordinates (ξ, η, ϕ) are defined through

$$x = c\sqrt{(\xi^2 - 1)(1 - \eta^2)} \cos \phi, \quad (9a)$$

$$y = c\sqrt{(\xi^2 - 1)(1 - \eta^2)} \sin \phi, \quad (9b)$$

$$z = c\xi\eta, \quad (9c)$$

where $\xi \in [1, +\infty)$ is the radial variable, $\eta \in [-1, 1]$ is the angular variable, and $\phi \in [0, 2\pi]$ is the azimuthal variable, respectively. The prolate spheroid (8) is called the reference prolate spheroid of this coordinate system. The coordinate surface of constant ξ is a prolate spheroid confocal to the prolate spheroid (8), and such a confocal prolate spheroid, denoted by S_ξ , can be written in the Cartesian coordinates as

$$\frac{x^2 + y^2}{c^2(\xi^2 - 1)} + \frac{z^2}{c^2\xi^2} = 1. \quad (10)$$

In particular, $\xi = \xi_b$ with $\xi_b = b/c$ is the prolate spheroid (8), and $\xi = 1$ corresponds to the focal line connecting the two focal points, respectively. The coordinate surfaces of constant η are the two sheets of a hyperboloid of revolution with focal points $z = \pm c$, and in particular $\eta = 1$, $\eta = -1$, and $\eta = 0$ correspond to the positive z -axis beyond the focal point $(0, 0, c)$, the negative z -axis beyond the focal point $(0, 0, -c)$, and the xy -plane, respectively. The coordinate surface of constant ϕ is a plane through the z -axis at an angle ϕ to the xz -plane. The metric coefficients for the prolate spheroidal coordinates are given by

$$h_\xi(\xi, \eta) = c\sqrt{\frac{(\xi^2 - \eta^2)}{(\xi^2 - 1)}}, \quad (11a)$$

$$h_\eta(\xi, \eta) = c\sqrt{\frac{(\xi^2 - \eta^2)}{(1 - \eta^2)}}, \quad (11b)$$

$$h_\phi(\xi, \eta) = c\sqrt{(\xi^2 - 1)(1 - \eta^2)}. \quad (11c)$$

The interior prolate spheroidal harmonics are $P_n^m(\xi)P_n^m(\eta) \cos m\phi$ and $P_n^m(\xi)P_n^m(\eta) \sin m\phi$, and the exterior prolate spheroidal harmonics are $Q_n^m(\xi)P_n^m(\eta) \cos m\phi$ and $Q_n^m(\xi)P_n^m(\eta) \sin m\phi$, for $n = 0, 1, \dots$ and $m = 0, 1, \dots, n$, where $P_n^m(x)$ and $Q_n^m(x)$ are the associated Legendre functions of the first and second kinds, respectively. In particular, $P_n^0(x) \equiv P_n(x)$ and $Q_n^0(x) \equiv Q_n(x)$ are the Legendre functions of the first and second kinds, respectively. Accordingly, the surface prolate spheroidal harmonics are $C_n^m(\eta, \phi) = P_n^m(\eta) \cos m\phi$ and $S_n^m(\eta, \phi) = P_n^m(\eta) \sin m\phi$, for $n = 0, 1, \dots$ and $m = 0, 1, \dots, n$, which are orthogonal over a confocal prolate spheroid S_ξ with respect to the following geometrical weighting function:

$$w_\xi(\eta) = \frac{1}{c^2\sqrt{(\xi^2 - \eta^2)(\xi^2 - 1)}}. \quad (12)$$

In fact, we have the following orthogonality relation:

$$\oint_{S_\xi} S_n^m(\eta, \phi) S_N^M(\eta, \phi) w_\xi(\eta) ds_\xi(\eta, \phi) \quad (13a)$$

$$= \gamma_{mn} \delta_{nN} \delta_{mM}, \quad (M > 0, m > 0),$$

$$\oint_{S_\xi} S_n^m(\eta, \phi) C_N^M(\eta, \phi) w_\xi(\eta) ds_\xi(\eta, \phi) = 0, \quad (13b)$$

$$\oint_{S_\xi} C_n^m(\eta, \phi) C_N^M(\eta, \phi) w_\xi(\eta) ds_\xi(\eta, \phi) \quad (13c)$$

$$= \gamma_{mn} \delta_{nN} \delta_{mM},$$

where δ_{ij} is the Kronecker delta, the differential surface element on S_ξ is

$$ds_\xi(\eta, \phi) = h_\eta h_\phi d\eta d\phi = \frac{1}{w_\xi(\eta)} d\eta d\phi, \quad (14)$$

and the normalization constants γ_{mn} are

$$\gamma_{mn} = \frac{2(n+m)!}{(2n+1)(n-m)!} (1 + \delta_{m0}) \pi. \quad (15)$$

The surface prolate spheroidal harmonics form a complete set of eigenfunctions over a prolate spheroid S_ξ . Therefore, any smooth function f defined over the prolate spheroid S_ξ can be expanded in terms of the surface prolate spheroidal harmonics. Furthermore, if f is even with respect to ϕ , then it can be expanded in terms of only the even surface prolate spheroidal harmonics; namely,

$$f(\eta, \phi) = \sum_{n=0}^{\infty} \sum_{m=0}^n c_{mn} C_n^m(\eta, \phi), \quad (16)$$

with the coefficients c_{mn} given by

$$c_{mn} = \frac{1}{\gamma_{mn}} \oint_{S_\xi} w_\xi(\eta) f(\eta, \phi) C_n^m(\eta, \phi) ds_\xi(\eta, \phi). \quad (17)$$

Finally, the expansion of $1/|\mathbf{r} - \mathbf{r}_s|$ in the prolate spheroidal coordinates is [1, 14, 15]

$$\frac{1}{|\mathbf{r} - \mathbf{r}_s|} = \frac{1}{c} \sum_{n=0}^{\infty} \sum_{m=0}^n H_{nm} P_n^m(\xi_c) Q_n^m(\xi_s) P_n^m(\eta_s) P_n^m(\eta) \cdot \cos m(\phi - \phi_s), \quad (18)$$

where $\xi_c = \min(\xi, \xi_s)$, $\xi_s = \max(\xi, \xi_s)$, and

$$H_{nm} = (2n+1)(2 - \delta_{m0}) (-1)^m \left[\frac{(n-m)!}{(n+m)!} \right]^2. \quad (19)$$

3. Interior Neumann Functions and Their Image Systems

Given a unit source located at point $\mathbf{r}_s = (x_s, y_s, z_s) = (\xi_s, \eta_s, \phi_s)$ inside the prolate spheroid S , that is, $1 \leq \xi_s < \xi_b$, we assume, without loss of any generality, that the source is in the xz -plane; that is, $y_s = \phi_s = 0$. We consider interior Neumann functions with several different Neumann boundary conditions.

3.1. Nonconstant Boundary Condition. The interior Neumann function considered in this case, denoted by $N_a^i(\mathbf{r}, \mathbf{r}_s)$, is the solution of the following boundary value problem:

$$\Delta N^i(\mathbf{r}, \mathbf{r}_s) = \delta(\mathbf{r} - \mathbf{r}_s), \quad 1 \leq \xi < \xi_b, \quad (20a)$$

$$\frac{\partial}{\partial n} N^i(\mathbf{r}, \mathbf{r}_s) = \frac{1}{4\pi} w_{\xi_b}(\eta), \quad \xi = \xi_b, \quad (20b)$$

where the normal derivative on S is set to be a constant multiple of the geometrical weighting function $w_{\xi}(\eta)$ on S . Compared to the boundary condition (3) which assumes a constant normal derivative on S , the boundary condition (20b) not only sounds more physical but also leads to a simpler mathematical formulation for the Neumann function. In fact, $1/|S|$ is the average of $(1/4\pi)w_{\xi_b}(\eta)$ on the prolate spheroid S since

$$\frac{1}{4\pi} \oint_S w_{\xi_b}(\eta) ds = 1. \quad (21)$$

This identity also guarantees that such a Neumann function exists. In this case, the weighted mean value of a function u on the surface S is $\langle u \rangle = \oint_S w_{\xi_b}(\eta) u(\mathbf{r}) ds / (4\pi)$.

Due to the azimuthal symmetry of the system, the interior Neumann function $N_a^i(\mathbf{r}, \mathbf{r}_s)$ can be expressed in terms of the even interior prolate spheroidal harmonics as

$$N_a^i(\mathbf{r}, \mathbf{r}_s) = -\frac{1}{4\pi |\mathbf{r} - \mathbf{r}_s|} + \frac{1}{4\pi c} \cdot \sum_{n=0}^{\infty} \sum_{m=0}^n A_{mn} H_{mn} P_n^m(\xi_s) P_n^m(\eta_s) P_n^m(\xi) C_n^m(\eta, \phi), \quad (22)$$

where A_{mn} are constants that have to be determined in such a way so as to satisfy the boundary condition (20b). Using (18), we can rewrite $N_a^i(\mathbf{r}, \mathbf{r}_s)$ in the neighborhood of the boundary S , where $\xi_s \leq \xi \leq \xi_b$, as

$$N_a^i(\mathbf{r}, \mathbf{r}_s) = -\frac{1}{4\pi c} \sum_{n=0}^{\infty} \sum_{m=0}^n H_{mn} P_n^m(\xi_s) P_n^m(\eta_s) \cdot [Q_n^m(\xi) - A_{mn} P_n^m(\xi)] C_n^m(\eta, \phi). \quad (23)$$

Since the surface normal derivative at any point (ξ_b, η, ϕ) on S is

$$\frac{\partial}{\partial n} = \frac{1}{h_{\xi}(\xi_b, \eta)} \frac{\partial}{\partial \xi} = \frac{a^2}{c} w_{\xi_b}(\eta) \frac{\partial}{\partial \xi}, \quad (24)$$

the boundary condition (20b) demands that the following equation holds at every point on S :

$$-\frac{a^2}{c^2} w_{\xi_b}(\eta) \sum_{n=0}^{\infty} \sum_{m=0}^n H_{mn} P_n^m(\xi_s) P_n^m(\eta_s) \cdot [Q_n^{m'}(\xi_b) - A_{mn} P_n^{m'}(\xi_b)] C_n^m(\eta, \phi) = w_{\xi_b}(\eta). \quad (25)$$

Obviously, A_{00} is the arbitrary constant of the solution $N_a^i(\mathbf{r}, \mathbf{r}_s)$ since $P_0'(x) \equiv 0$. Indeed, integrating (25) over S and

using the orthogonality relation (13a), (13b), and (13c), we obtain

$$Q_0'(\xi_b) = -\frac{c^2}{a^2}, \quad (26)$$

which is an identity that can be verified using $Q_0(x) = \ln((x+1)/(x-1))/2$.

Next, for each $i \geq 1$ and $j = 0, \dots, i$, multiplying both sides of (25) by $C_i^j(\eta, \phi)$, integrating it over S , and using the orthogonality relation (13a), (13b), and (13c), we obtain

$$-\frac{a^2}{c^2} \gamma_{ji} H_{ji} P_i^j(\xi_s) P_i^j(\eta_s) [Q_i^{j'}(\xi_b) - A_{ji} P_i^{j'}(\xi_b)] = \oint_S w_{\xi_b}(\eta) C_i^j(\eta, \phi) ds_{\xi_b}(\eta, \phi) = 0, \quad (27)$$

from which we get

$$A_{mn} = \frac{Q_n^{m'}(\xi_b)}{P_n^{m'}(\xi_b)}, \quad n \geq 1. \quad (28)$$

Hence, the interior Neumann function $N_a^i(\mathbf{r}, \mathbf{r}_s)$ is

$$N_a^i(\mathbf{r}, \mathbf{r}_s) = -\frac{1}{4\pi |\mathbf{r} - \mathbf{r}_s|} + \frac{A_{00}}{4\pi c} + \frac{1}{4\pi c} \sum_{n=1}^{\infty} \sum_{m=0}^n H_{nm} \cdot \frac{Q_n^{m'}(\xi_b)}{P_n^{m'}(\xi_b)} P_n^m(\xi_s) P_n^m(\eta_s) P_n^m(\xi) C_n^m(\eta, \phi). \quad (29)$$

The arbitrary constant A_{00} may be fixed by demanding one additional condition, say $N_a^i(\mathbf{0}, \mathbf{r}_s) = 0$. In this case, noting that the origin in the prolate spheroidal coordinates corresponds to the point $(1, 0, 0)$ and that

$$P_n^m(\pm 1) = \begin{cases} (\pm 1)^n, & \text{if } m = 0, \\ 0, & \text{if } m > 0, \end{cases} \quad (30)$$

$$P_n(0) = \begin{cases} (-1)^{n/2} \frac{(n-1)!!}{n!!}, & \text{if } n \text{ is even,} \\ 0, & \text{if } n \text{ is odd,} \end{cases}$$

we get

$$A_{00} = \frac{c}{|\mathbf{r}_s|} - \sum_{k=1}^{\infty} (4k+1) \frac{Q_{2k}'(\xi_b)}{P_{2k}'(\xi_b)} P_{2k}(\xi_s) P_{2k}(\eta_s) (-1)^k \cdot \frac{(2k-1)!!}{(2k)!!}. \quad (31)$$

3.2. Constant Nonzero Boundary Condition. The interior Neumann function with a constant nonzero normal derivative on S , denoted by $N_b^i(\mathbf{r}, \mathbf{r}_s)$, is defined as the solution of the differential equation (20a) with the boundary condition

$$\frac{\partial}{\partial n} N^i(\mathbf{r}, \mathbf{r}_s) = \frac{1}{|S|}, \quad \xi = \xi_b, \quad (32)$$

where $|S|$ stands for the total surface area of S . In this case, the term $\langle u \rangle$ in (5) is the average value of the solution u on S ; namely, $\langle u \rangle = \oint_S u(\mathbf{r}) ds / |S|$.

The interior Neumann function $N_b^i(\mathbf{r}, \mathbf{r}_s)$ is also given by (22), but now the boundary condition (32) demands that the following equation holds at every point on S :

$$-\frac{a^2}{4\pi c^2} w_{\xi_b}(\eta) \sum_{n=0}^{\infty} \sum_{m=0}^n H_{nm} P_n^m(\xi_s) P_n^m(\eta_s) \cdot [Q_n^{m'}(\xi_b) - A_{nm} P_n^{m'}(\xi_b)] C_n^m(\eta, \phi) = \frac{1}{|S|}. \quad (33)$$

Clearly, A_{00} still serves as the arbitrary constant of the interior Neumann function. Indeed, integrating (33) over S and using (13a), (13b), and (13c), we still have identity (26). Next, for each $i \geq 1$ and $j = 0, \dots, i$, multiplying both sides of (33) by $C_i^j(\eta, \phi)$, integrating it over S , and using the orthogonality relation (13a), (13b), and (13c), we obtain

$$-\frac{a^2}{4\pi c^2} \gamma_{ji} H_{ji} P_i^j(\xi_s) P_i^j(\eta_s) [Q_i^{j'}(\xi_b) - A_{ji} P_i^{j'}(\xi_b)] = \frac{1}{|S|} \oint_S C_i^j(\eta, \phi) ds_{\xi_b}(\eta, \phi). \quad (34)$$

The right-hand side of (34), however, is no longer zero for all $i \geq 1$ and $j = 0, \dots, i$. Instead, noting that

$$\oint_S C_i^j(\eta, \phi) ds_{\xi_b}(\eta, \phi) = ac \int_{-1}^1 P_i^j(\eta) \sqrt{\xi_b^2 - \eta^2} d\eta \int_0^{2\pi} \cos(j\phi) d\phi, \quad (35)$$

we have

$$\oint_S C_i^j(\eta, \phi) ds_{\xi_b}(\eta, \phi) = \begin{cases} 2\pi ac \int_{-1}^1 P_i(\eta) \sqrt{\xi_b^2 - \eta^2} d\eta, & \text{if } j = 0, i \text{ is even,} \\ 0, & \text{otherwise.} \end{cases} \quad (36)$$

Therefore, when $m > 0$ or when $m = 0$ and $n \geq 1$ is odd, we still have (28), but when $m = 0$ and $n \geq 1$ is even, we instead have

$$A_{0n} = \frac{Q_n'(\xi_b)}{P_n'(\xi_b)} + \frac{2\pi c^3 \int_{-1}^1 P_n(\eta) \sqrt{\xi_b^2 - \eta^2} d\eta}{a |S| P_n(\xi_s) P_n(\eta_s) P_n'(\xi_b)}. \quad (37)$$

3.3. Homogeneous Boundary Condition. If we demand the homogeneous boundary condition on S , then the interior Neumann function, denoted by $N_c^i(\mathbf{r}, \mathbf{r}_s)$, is defined as the solution of the following boundary value problem [16]:

$$\Delta N^i(\mathbf{r}, \mathbf{r}_s) = \delta(\mathbf{r} - \mathbf{r}_s) - 1/|\Omega|, \quad 1 \leq \xi < \xi_b, \quad (38a)$$

$$\frac{\partial}{\partial n} N^i(\mathbf{r}, \mathbf{r}_s) = 0, \quad \xi = \xi_b, \quad (38b)$$

where $|\Omega| = (4\pi/3)a^2b$ stands for the volume of Ω . The extra term $1/|\Omega|$ in the differential equation (38a) is needed to guarantee the existence of such a Neumann function, and in this case the solution to the Neumann problem (4a) and (4b) is still given by (5) but with the term $\langle u \rangle$ representing the average value of the solution u in the volume Ω ; namely, $\langle u \rangle = \int_{\Omega} u(\mathbf{r}) d\mathbf{r} / |\Omega|$.

Let $u_0(\mathbf{r})$ be a function in Ω defined as

$$u_0(\mathbf{r}) = \frac{r^2}{6|\Omega|} = \frac{x^2 + y^2 + z^2}{6|\Omega|} = \frac{c^2(\xi^2 + \eta^2 - 1)}{8\pi a^2 b}. \quad (39)$$

Then, it is easy to see that $\Delta u_0(\mathbf{r}) = 1/|\Omega|$ and that

$$\begin{aligned} \frac{\partial}{\partial n} u_0(\mathbf{r}) \Big|_{\xi=\xi_b} &= \frac{1}{8\pi a^2 b} \frac{a^2}{c} w_{\xi_b}(\eta) \frac{\partial}{\partial \xi} [c^2(\xi^2 + \eta^2 - 1)] \Big|_{\xi=\xi_b} \\ &= \frac{1}{4\pi} w_{\xi_b}(\eta). \end{aligned} \quad (40)$$

Therefore, the Neumann function $N_c^i(\mathbf{r}, \mathbf{r}_s)$ can be obtained by subtracting $u_0(\mathbf{r})$ from the Neumann function $N_a^i(\mathbf{r}, \mathbf{r}_s)$; namely, we have

$$N_c^i(\mathbf{r}, \mathbf{r}_s) = N_a^i(\mathbf{r}, \mathbf{r}_s) - \frac{r^2}{6|\Omega|}. \quad (41)$$

3.4. Image Systems for Interior Neumann Functions. Let us now turn to the construction of image systems for the interior Neumann functions. We will focus ourselves on the interior Neumann function $N_a^i(\mathbf{r}, \mathbf{r}_s)$ given by (29), but the basic idea and the key conclusions apply to other interior Neumann functions as well.

More specifically, we wish to build an image system that represents the following part of the interior Neumann function $N_a^i(\mathbf{r}, \mathbf{r}_s)$:

$$N_a^{i,\text{ref}}(\mathbf{r}, \mathbf{r}_s) = \frac{1}{4\pi c} \sum_{n=1}^{\infty} \sum_{m=0}^n H_{nm} \frac{Q_n^{m'}(\xi_b)}{P_n^{m'}(\xi_b)} P_n^m(\xi_s) \cdot P_n^m(\eta_s) P_n^m(\xi) C_n^m(\eta, \phi). \quad (42)$$

As pointed out earlier, such an image system is not unique. By reasoning as Dassios and Sten did in the case of the ellipsoidal geometry [12], here we consider an image system consisting of a point image with strength Q at some exterior point $\mathbf{r}_k = (x_k, 0, z_k) = (\xi_k, \eta_k, 0)$ (since the source is in the xz -plane, naturally the only point image should be in the xz -plane as well) as a continuous one-dimensional line image extending from the point \mathbf{r}_k to infinity along the radial coordinate curve $C : (\eta, \phi) = (\eta_k, 0)$ with density

$$\rho(\mathbf{t}) = \rho(\xi, \eta_k, 0) = \frac{\alpha q(\xi)}{h_{\xi}(\xi, \eta_k)}, \quad (43)$$

where α is some constant and $q(\xi)$ is some continuous function in $[\xi_k, +\infty)$, and as a continuous two-dimensional

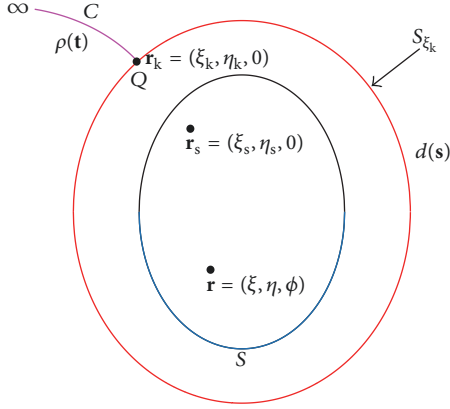


FIGURE 2: Illustration of the image system for the interior Neumann function $N_a^i(\mathbf{r}, \mathbf{r}_s)$.

surface image on the confocal prolate spheroid $S_{\xi_k} : \xi = \xi_k$ with density

$$d(\mathbf{s}) = d(\xi_k, \eta, \phi) = w_{\xi_k}(\eta) \sum_{n=2}^{\infty} \sum_{m=0}^n d_{mn} C_n^m(\eta, \phi), \quad (44)$$

where d_{mn} are constants to be determined later. By reasoning as we did in the case of Dirichlet-Green's function [11], the vanishing of the $n = 0$ term in $d(\mathbf{s})$ implies that the total strength (or in electrostatics, the total surface "charge") on S_{ξ_k} is zero, and the vanishing of the $n = 1$ terms in $d(\mathbf{s})$ implies that the distribution on S_{ξ_k} is symmetric with its centroid at the origin. Such an image system is graphically illustrated in Figure 2.

As pointed out by Dassios [10], the existence of the continuous one-dimensional distribution of images in the proposed image system is characteristic of the Neumann boundary condition, which in fact was shown 70 years ago by Weiss who studied image systems through applications of Kelvin's transformation in electricity, magnetism, and hydrodynamics [17, 18]. Dassios further provided an intuitive explanation of the one-dimensional distribution of images reflecting the physics of the underlying problem, that is, the Neumann boundary condition. Since the derivative is the limit of the difference of the solution between two points and the image interpretation of such difference demands a sequence of point images with gaps that are proportional to the distance between the two points, it then becomes clear that the set of point images evolves into a continuous curve as the two points approach each other in order to define the derivative. On the other hand, the existence of the continuous two-dimensional distribution of images over a closed surface in the image system is a direct consequence of the three-dimensional character of the spheroidal or ellipsoidal geometry as it compares with the essentially one-dimensional character of the spherical geometry in which, as mentioned in Section 1, point and line images are enough to represent interior Neumann functions.

The potential in the interior of the spheroid S generated by this image system is

$$N_a^{i,\text{im}}(\mathbf{r}) = -\frac{Q}{4\pi |\mathbf{r} - \mathbf{r}_k|} - \frac{1}{4\pi} \int_C \frac{\rho(\mathbf{t}')}{|\mathbf{r} - \mathbf{t}'|} dl(\mathbf{t}') - \frac{1}{4\pi} \oint_{S_{\xi_k}} \frac{d(\mathbf{s}')}{|\mathbf{r} - \mathbf{s}'|} ds_{\xi_k}(\eta', \phi'), \quad (45)$$

where $\mathbf{t}' = (\xi', \eta_k, 0)$, $\mathbf{s}' = (\xi_k, \eta', \phi')$, and $dl(\mathbf{t}')$ is the differential length element on C ; that is, $dl(\mathbf{t}') = h_{\xi}(\xi', \eta_k) d\xi'$. Therefore, we have

$$N_a^{i,\text{im}}(\mathbf{r}) = -\frac{Q}{4\pi |\mathbf{r} - \mathbf{r}_k|} - \frac{\alpha}{4\pi} \int_{\xi_k}^{+\infty} \frac{q(\xi')}{|\mathbf{r} - \mathbf{t}'|} d\xi' - \frac{1}{4\pi} \oint_{S_{\xi_k}} \frac{d(\xi_k, \eta', \phi')}{|\mathbf{r} - \mathbf{s}'|} ds_{\xi_k}(\eta', \phi'). \quad (46)$$

Using (18), we have

$$\begin{aligned} \frac{Q}{4\pi |\mathbf{r} - \mathbf{r}_k|} &= \frac{Q}{4\pi c} \sum_{n=0}^{\infty} \sum_{m=0}^n H_{mn} Q_n^m(\xi_k) P_n^m(\eta_k) P_n^m(\xi) \\ &\cdot C_n^m(\eta, \phi), \\ \frac{\alpha}{4\pi} \int_{\xi_k}^{+\infty} \frac{q(\xi')}{|\mathbf{r} - \mathbf{t}'|} d\xi' &= \frac{1}{4\pi c} \\ &\cdot \sum_{n=0}^{\infty} \sum_{m=0}^n H_{mn} \left(\alpha \int_{\xi_k}^{+\infty} q(\xi') Q_n^m(\xi') d\xi' \right) P_n^m(\eta_k) \\ &\cdot P_n^m(\xi) C_n^m(\eta, \phi). \end{aligned} \quad (47)$$

Furthermore, using (18), (44), and the orthogonality relation (13a), (13b), and (13c), we obtain

$$\begin{aligned} \frac{1}{4\pi} \oint_{S_{\xi_k}} \frac{d(\xi_k, \eta', \phi')}{|\mathbf{r} - \mathbf{s}'|} ds_{\xi_k}(\eta', \phi') \\ = \frac{1}{4\pi c} \sum_{n=2}^{\infty} \sum_{m=0}^n H_{mn} \gamma_{mn} d_{mn} Q_n^m(\xi_k) P_n^m(\xi) C_n^m(\eta, \phi). \end{aligned} \quad (48)$$

So, demanding $N_a^{i,\text{ref}}(\mathbf{r}, \mathbf{r}_s) = N_a^{i,\text{im}}(\mathbf{r})$, we have

$$\begin{aligned} \frac{1}{4\pi c} \sum_{n=0}^{\infty} \sum_{m=0}^n H_{mn} \left[Q Q_n^m(\xi_k) \right. \\ \left. + \alpha \int_{\xi_k}^{+\infty} q(\xi') Q_n^m(\xi') d\xi' \right] P_n^m(\eta_k) P_n^m(\xi) \\ \cdot C_n^m(\eta, \phi) + \frac{1}{4\pi c} \sum_{n=2}^{\infty} \sum_{m=0}^n H_{mn} \gamma_{mn} d_{mn} Q_n^m(\xi_k) \\ \cdot P_n^m(\xi) C_n^m(\eta, \phi) = -\frac{1}{4\pi c} \sum_{n=1}^{\infty} \sum_{m=0}^n H_{mn} \\ \cdot \frac{Q_n^m(\xi_b)}{P_n^m(\xi_b)} P_n^m(\xi_s) P_n^m(\eta_s) P_n^m(\xi) C_n^m(\eta, \phi). \end{aligned} \quad (49)$$

First, comparing the monopole ($n = 0$) term in both sides of (49), we have

$$QQ_0(\xi_k) + \alpha \int_{\xi_k}^{+\infty} q(\xi') Q_0(\xi') d\xi' = 0, \quad (50)$$

from which we get

$$Q = -\frac{\alpha}{Q_0(\xi_k)} \int_{\xi_k}^{+\infty} q(\xi') Q_0(\xi') d\xi'. \quad (51)$$

The function $q(\xi)$ in $[\xi_k, +\infty)$ is something one can choose as long as the corresponding improper integrals in (49) all exist. For instance, we can choose

$$q(\xi) = 1 - \frac{1}{\xi Q_0(\xi)}. \quad (52)$$

In this case, the fact that the improper integral in (51) exists can be verified straightforwardly and the fact that the improper integrals in (49) for $n \geq 1$ all exist is due to $Q_n^m(\xi) = O(1/\xi^{n+1})$ as $\xi \rightarrow +\infty$. In fact, we have

$$\begin{aligned} & \int_{\xi_k}^{+\infty} q(\xi') Q_0(\xi') d\xi' \\ &= \frac{\xi_k}{2} \ln \left(\frac{\xi_k + 1}{\xi_k - 1} \right) + \frac{1}{2} \ln \left(\frac{\xi_k^2 - 1}{\xi_k^2} \right) - 1. \end{aligned} \quad (53)$$

Next, comparing the dipole ($n = 1$) terms in both sides of (49), we obtain for $m = 0, 1$

$$\begin{aligned} & \alpha \int_{\xi_k}^{+\infty} q(\xi') \left[Q_1^m(\xi') - \frac{Q_1^m(\xi_k)}{Q_0(\xi_k)} \right. \\ & \quad \left. \cdot Q_0(\xi') \right] d\xi' P_1^m(\eta_k) \\ &= -\frac{Q_1^{m'}(\xi_b)}{P_1^{m'}(\xi_b)} P_1^m(\xi_s) P_1^m(\eta_s). \end{aligned} \quad (54)$$

Using (9a), (9b), and (9c) and noting that $\phi_k = \phi_s = 0$, we obtain

$$x_k = -\frac{P_1^1(\xi_k)}{\alpha g_1^1(\xi_k)} \frac{Q_1^1(\xi_b)}{P_1^1(\xi_b)} x_s, \quad (55a)$$

$$z_k = -\frac{P_1(\xi_k)}{\alpha g_1(\xi_k)} \frac{Q_1'(\xi_b)}{P_1'(\xi_b)} z_s, \quad (55b)$$

where $g_1(\xi_k) \equiv g_1^0(\xi_k)$ and

$$g_1^m(\xi_k) = \int_{\xi_k}^{+\infty} q(\xi') \left[Q_1^m(\xi') - \frac{Q_1^m(\xi_k)}{Q_0(\xi_k)} Q_0(\xi') \right] d\xi', \quad (56)$$

$$m = 0, 1.$$

Since the point image Q lies on the confocal prolate spheroid S_{ξ_k} , we obtain

$$\begin{aligned} & \frac{x_s^2}{c^2(\xi_k^2 - 1)} \frac{P_1^1(\xi_k)^2}{\alpha^2 g_1^1(\xi_k)^2} \frac{Q_1^1(\xi_b)^2}{P_1^1(\xi_b)^2} \\ & + \frac{z_s^2}{c^2 \xi_k^2} \frac{P_1(\xi_k)^2}{\alpha^2 g_1(\xi_k)^2} \frac{Q_1'(\xi_b)^2}{P_1'(\xi_b)^2} = 1, \end{aligned} \quad (57)$$

which can be rewritten as

$$\begin{aligned} & \frac{x_s^2}{a^2} \frac{P_1^1(\xi_b)^2}{\alpha^2 g_1^1(\xi_k)^2} \frac{Q_1^1(\xi_b)^2}{P_1^1(\xi_b)^2} + \frac{z_s^2}{b^2} \frac{P_1(\xi_b)^2}{\alpha^2 g_1(\xi_k)^2} \frac{Q_1'(\xi_b)^2}{P_1'(\xi_b)^2} \\ & = 1. \end{aligned} \quad (58)$$

Equation (58) provides us with a nonlinear algebraic equation for the radial coordinate ξ_k of the point image Q . Unfortunately, this equation does not necessarily have a solution in $(\xi_b, +\infty)$. However, if we choose the constant α as one satisfying

$$\begin{aligned} \alpha^2 = \beta^2 & \left[\frac{x_s^2}{a^2} \frac{P_1^1(\xi_b)^2}{g_1^1(\xi_b)^2} \frac{Q_1^1(\xi_b)^2}{P_1^1(\xi_b)^2} \right. \\ & \left. + \frac{z_s^2}{b^2} \frac{P_1(\xi_b)^2}{g_1(\xi_b)^2} \frac{Q_1'(\xi_b)^2}{P_1'(\xi_b)^2} \right], \end{aligned} \quad (59)$$

where β is a constant such that $\beta^2 > 1$, then (58) has a solution in $(\xi_b, +\infty)$. Indeed, define an auxiliary function $f(\xi) : (\xi_b, +\infty) \rightarrow \mathbb{R}$ as

$$\begin{aligned} f(\xi) = & \frac{x_s^2}{a^2} \frac{P_1^1(\xi_b)^2}{\alpha^2 g_1^1(\xi)^2} \frac{Q_1^1(\xi_b)^2}{P_1^1(\xi_b)^2} \\ & + \frac{z_s^2}{b^2} \frac{P_1(\xi_b)^2}{\alpha^2 g_1(\xi)^2} \frac{Q_1'(\xi_b)^2}{P_1'(\xi_b)^2} - 1. \end{aligned} \quad (60)$$

First, it can be demonstrated that $f(\xi)$ is continuous on $(\xi_b, +\infty)$. Then, note that, for $m = 0, 1$, as $\xi \rightarrow +\infty$, we have $g_1^m(\xi) \rightarrow 0$ and thus $f(\xi) \rightarrow +\infty$. Next, it is easy to see that $f(\xi_b) = 1/\beta^2 - 1 < 0$. Therefore, (58) must have a solution in $(\xi_b, +\infty)$. In addition, we note that the constant β should be chosen in such a way so as to guarantee that the point image is close to the boundary if the source is close to the boundary. For example, we can choose $\beta = (\xi_b/\xi_s)^m$ or $\beta = (Q_0(\xi_s)/Q_0(\xi_b))^m$ for some constant $m > 0$.

We were unable to prove the uniqueness of such a solution, but numerical investigations have suggested that the solution of (58) in $(\xi_b, +\infty)$ should be unique. Figure 3 shows the graph of $f(\xi)$ for the case of $a = 1$, $b = 2$ (so $\xi_b = 2/\sqrt{3}$), and $\mathbf{r}_s = (0.5, 0, 1)$ with $\beta = Q_0(\xi_s)/Q_0(\xi_b)$. In this case, the unique solution is about 1.197158. In general, Newton's method can be used to solve (58) for ξ_k . Once ξ_k is found, we can use (55a) and (55b) to calculate x_k and z_k and consequently η_k , and we can use (51) to calculate the strength Q of the point image, respectively.

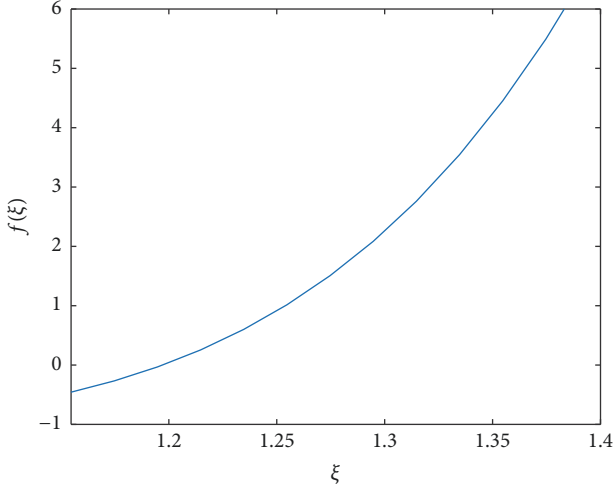


FIGURE 3: The graph of $f(\xi)$ for the case of $a = 1$, $b = 2$, and $\mathbf{r}_s = (0.5, 0, 1)$.

Finally, comparing the $n \geq 2$ terms in both sides of (49), we obtain

$$\begin{aligned} \gamma_{mn} d_{mn} Q_n^m(\xi_k) &= -\frac{Q_n^{m'}(\xi_b)}{P_n^{m'}(\xi_b)} P_n^m(\xi_s) P_n^m(\eta_s) \\ &\quad - \left[QQ_n^m(\xi_k) + \alpha \int_{\xi_k}^{+\infty} q(\xi') Q_n^m(\xi') d\xi' \right] \\ &\quad \cdot P_n^m(\eta_k). \end{aligned} \quad (61)$$

Therefore, the coefficients of the surface image density (44) are given by

$$\begin{aligned} d_{mn} &= \frac{-1}{\gamma_{mn} Q_n^m(\xi_k)} \left\{ \frac{Q_n^{m'}(\xi_b)}{P_n^{m'}(\xi_b)} P_n^m(\xi_s) P_n^m(\eta_s) \right. \\ &\quad + \left[QQ_n^m(\xi_k) + \alpha \int_{\xi_k}^{+\infty} q(\xi') Q_n^m(\xi') d\xi' \right] \\ &\quad \left. \cdot P_n^m(\eta_k) \right\}. \end{aligned} \quad (62)$$

4. Exterior Neumann Functions and Their Image Systems

Given a unit source located at point $\mathbf{r}_s = (x_s, y_s, z_s) = (\xi_s, \eta_s, \phi_s)$ outside the prolate spheroid S , so $\xi_s > \xi_b > 1$. Again, we assume the source is in the xz -plane so $y_s = \phi_s = 0$. We shall consider exterior Neumann functions with several different boundary conditions as well.

4.1. Nonconstant Boundary Condition. The exterior Neumann function considered in this case, denoted by $N_a^e(\mathbf{r}, \mathbf{r}_s)$,

is the solution of the following boundary value problem:

$$\Delta N^e(\mathbf{r}, \mathbf{r}_s) = \delta(\mathbf{r} - \mathbf{r}_s), \quad \xi > \xi_b, \quad (63a)$$

$$\frac{\partial}{\partial n} N^e(\mathbf{r}, \mathbf{r}_s) = -\frac{1}{4\pi} w_{\xi_b}(\eta), \quad \xi = \xi_b, \quad (63b)$$

$$N^e(\mathbf{r}, \mathbf{r}_s) = O(1/|\mathbf{r}|^2), \quad |\mathbf{r}| \rightarrow +\infty. \quad (63c)$$

Due to the azimuthal symmetry of the system, the exterior Neumann function $N_a^e(\mathbf{r}, \mathbf{r}_s)$ can be expressed in terms of the even exterior prolate spheroidal harmonics as

$$\begin{aligned} N_a^e(\mathbf{r}, \mathbf{r}_s) &= -\frac{1}{4\pi |\mathbf{r} - \mathbf{r}_s|} + \frac{1}{4\pi c} \\ &\quad \cdot \sum_{n=0}^{\infty} \sum_{m=0}^n B_{mn} H_{mn} Q_n^m(\xi_s) P_n^m(\eta_s) Q_n^m(\xi) C_n^m(\eta, \phi), \end{aligned} \quad (64)$$

where B_{mn} are constants that have to be determined by the boundary condition (63b). Using (18), we can rewrite $N_a^e(\mathbf{r}, \mathbf{r}_s)$ in the neighborhood of the boundary S , where $\xi_b \leq \xi \leq \xi_s$, as

$$\begin{aligned} N_a^e(\mathbf{r}, \mathbf{r}_s) &= -\frac{1}{4\pi c} \sum_{n=0}^{\infty} \sum_{m=0}^n H_{mn} Q_n^m(\xi_s) P_n^m(\eta_s) \\ &\quad \cdot [P_n^m(\xi) - B_{mn} Q_n^m(\xi)] C_n^m(\eta, \phi). \end{aligned} \quad (65)$$

The boundary condition (63b) demands that the following equation holds at every point on S :

$$\begin{aligned} \frac{a^2}{c^2} w_{\xi_b}(\eta) \sum_{n=0}^{\infty} \sum_{m=0}^n H_{mn} Q_n^m(\xi_s) P_n^m(\eta_s) \\ \cdot [P_n^{m'}(\xi_b) - B_{mn} Q_n^{m'}(\xi_b)] C_n^m(\eta, \phi) = w_{\xi_b}(\eta). \end{aligned} \quad (66)$$

Integrating (66) over S and using the orthogonality relation (13a), (13b), and (13c), we obtain

$$\begin{aligned} -\frac{a^2}{c^2} \gamma_{00} H_{00} Q_0(\xi_s) P_0(\eta_s) Q_0'(\xi_b) B_{00} \\ = \oint_S w_{\xi_b}(\eta) ds_{\xi_b}(\eta, \phi) = \gamma_{00}. \end{aligned} \quad (67)$$

Therefore, we have

$$B_{00} = -\frac{c^2}{a^2 Q_0(\xi_s) P_0(\eta_s) Q_0'(\xi_b)} = \frac{1}{Q_0(\xi_s)}. \quad (68)$$

Next, for each $i \geq 1$ and $j = 0, \dots, i$, multiplying both sides of (66) by $C_i^j(\eta, \phi)$, integrating it over S , and using (13a), (13b), and (13c), we obtain

$$\begin{aligned} \frac{a^2}{c^2} \gamma_{ji} H_{ji} Q_i^j(\xi_s) P_i^j(\eta_s) [P_i^{j'}(\xi_b) - B_{ji} Q_i^{j'}(\xi_b)] \\ = \oint_S w_{\xi_b}(\eta) C_i^j(\eta, \phi) ds_{\xi_b}(\eta, \phi) = 0, \end{aligned} \quad (69)$$

from which we get

$$B_{mn} = \frac{P_n^{m'}(\xi_b)}{Q_n^{m'}(\xi_b)}, \quad n \geq 1. \quad (70)$$

Hence, the exterior Neumann function $N_a^e(\mathbf{r}, \mathbf{r}_s)$ is given by

$$N_a^e(\mathbf{r}, \mathbf{r}_s) = -\frac{1}{4\pi|\mathbf{r}-\mathbf{r}_s|} + \frac{Q_0(\xi)}{4\pi c} + \frac{1}{4\pi c} \sum_{n=1}^{\infty} \sum_{m=0}^n H_{mn} \cdot \frac{P_n^{m'}(\xi_b)}{Q_n^{m'}(\xi_b)} Q_n^m(\xi_s) P_n^m(\eta_s) Q_n^m(\xi) C_n^m(\eta, \phi). \quad (71)$$

4.2. Constant Nonzero Boundary Condition. The exterior Neumann function with a constant nonzero normal derivative on S , denoted by $N_b^e(\mathbf{r}, \mathbf{r}_s)$, is defined as the solution of the differential equation (63a) with the boundary conditions (63c) and

$$\frac{\partial}{\partial n} N^e(\mathbf{r}, \mathbf{r}_s) = -\frac{1}{|S|}, \quad \xi = \xi_b. \quad (72)$$

In this case, the exterior Neumann function $N_b^e(\mathbf{r}, \mathbf{r}_s)$ is still given by (64), but now the boundary condition (72) demands that the following equation holds at every point on S :

$$\frac{a^2}{4\pi c^2} \omega_{\xi_b}(\eta) \sum_{n=0}^{\infty} \sum_{m=0}^n H_{mn} Q_n^m(\xi_s) P_n^m(\eta_s) \cdot [P_n^{m'}(\xi_b) - B_{mn} Q_n^{m'}(\xi_b)] C_n^m(\eta, \phi) = \frac{1}{|S|}. \quad (73)$$

Integrating (73) over S and using the orthogonality relation (13a), (13b), and (13c), we obtain

$$-\frac{a^2}{4\pi c^2} \gamma_{00} H_{00} Q_0(\xi_s) P_0(\eta_s) Q_0'(\xi_b) B_{00} = \frac{1}{|S|} \oint_S ds_{\xi_b}(\eta, \phi) = 1. \quad (74)$$

Therefore, we still have $B_{00} = 1/Q_0(\xi_s)$. Next, for each $i \geq 1$ and $j = 0, \dots, i$, multiplying both sides of (73) by $C_i^j(\eta, \phi)$, integrating it over S , and using (13a), (13b), and (13c), we obtain

$$\frac{a^2}{4\pi c^2} \gamma_{ji} H_{ji} Q_i^j(\xi_s) P_i^j(\eta_s) [P_i^{j'}(\xi_b) - B_{ji} Q_i^{j'}(\xi_b)] = \frac{1}{|S|} \oint_S C_i^j(\eta, \phi) ds_{\xi_b}(\eta, \phi). \quad (75)$$

As shown by (36), the right-hand side of (75) is no longer zero for all $i \geq 1$ and $j = 0, \dots, i$. When $m > 0$ or when $m = 0$ and $n \geq 1$ is odd, we still have (70); however, when $m = 0$ and $n \geq 1$ is even, we instead have

$$B_{0n} = \frac{P_n'(\xi_b)}{Q_n'(\xi_b)} - \frac{2\pi c^3 \int_{-1}^1 P_n(\eta) \sqrt{\xi_b^2 - \eta^2} d\eta}{a|S| Q_n(\xi_s) P_n(\eta_s) Q_n'(\xi_b)}. \quad (76)$$

Note that (76) applies to the case of $n = m = 0$, yielding $B_{00} = 1/Q_0(\xi_s)$.

4.3. Homogeneous Boundary Condition. The exterior Neumann function with the homogeneous boundary condition on S , denoted by $N_c^e(\mathbf{r}, \mathbf{r}_s)$, is defined as the solution of the differential equation (63a) with the boundary conditions (63c) and

$$\frac{\partial}{\partial n} N^e(\mathbf{r}, \mathbf{r}_s) = 0, \quad \xi = \xi_b. \quad (77)$$

In this case, the exterior Neumann function $N_c^e(\mathbf{r}, \mathbf{r}_s)$ is still given by (64), but now the boundary condition (77) demands that the following equation holds at every point on S :

$$\frac{a^2}{4\pi c^2} \omega_{\xi_b}(\eta) \sum_{n=0}^{\infty} \sum_{m=0}^n H_{mn} Q_n^m(\xi_s) P_n^m(\eta_s) \cdot [P_n^{m'}(\xi_b) - B_{mn} Q_n^{m'}(\xi_b)] C_n^m(\eta, \phi) = 0, \quad (78)$$

from which we get $B_{00} = 0$ and (70). Therefore, the exterior Neumann function $N_c^e(\mathbf{r}, \mathbf{r}_s)$ is given by

$$N_c^e(\mathbf{r}, \mathbf{r}_s) = -\frac{1}{4\pi|\mathbf{r}-\mathbf{r}_s|} + \frac{1}{4\pi c} \sum_{n=1}^{\infty} \sum_{m=0}^n H_{mn} \cdot \frac{P_n^{m'}(\xi_b)}{Q_n^{m'}(\xi_b)} Q_n^m(\xi_s) P_n^m(\eta_s) Q_n^m(\xi) C_n^m(\eta, \phi). \quad (79)$$

4.4. Image Systems for Exterior Neumann Functions. Again, we will focus ourselves on an image system for the exterior Neumann function $N_a^e(\mathbf{r}, \mathbf{r}_s)$ given by (71). In particular, let us build an image system that can represent the reflected part of the Neumann function $N_a^e(\mathbf{r}, \mathbf{r}_s)$; namely,

$$N_a^{e,\text{ref}}(\mathbf{r}, \mathbf{r}_s) = \frac{Q_0(\xi)}{4\pi c} + \frac{1}{4\pi c} \sum_{n=1}^{\infty} \sum_{m=0}^n H_{mn} \cdot \frac{P_n^{m'}(\xi_b)}{Q_n^{m'}(\xi_b)} Q_n^m(\xi_s) P_n^m(\eta_s) Q_n^m(\xi) C_n^m(\eta, \phi). \quad (80)$$

First of all, the potential $Q_0(\xi)/(4\pi c)$ is generated by a focal line image of uniform density:

$$\mu(z) = -\frac{1}{2c}, \quad -c \leq z \leq c. \quad (81)$$

Indeed, the potential generated by this focal line image is

$$-\frac{1}{4\pi} \int_{-c}^c \frac{\mu(z)}{|\mathbf{r} - (0, z, 0)|} dz = \frac{1}{8\pi} \int_{-1}^1 \frac{1}{|\mathbf{r} - (1, \eta', 0)|} d\eta' = \frac{1}{8\pi c}$$

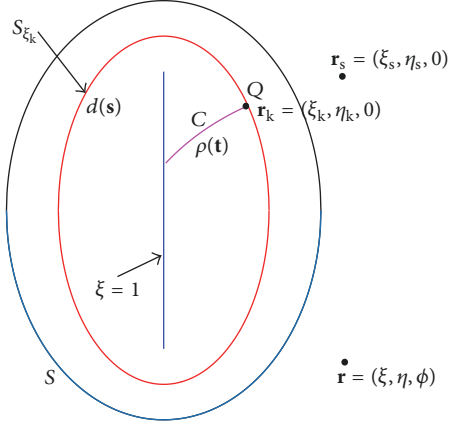


FIGURE 4: Illustration of the image system for the exterior Neumann function $N_a^e(\mathbf{r}, \mathbf{r}_s)$.

$$\begin{aligned} & \cdot \sum_{n=0}^{\infty} (2n+1) \left[\int_{-1}^1 P_n(\eta') d\eta' \right] P_n(1) Q_n(\xi) P_n(\eta) \\ &= \frac{Q_0(\xi)}{4\pi c}. \end{aligned} \quad (82)$$

The strength (or in electrostatics, the total “charge”) of this focal line image is

$$\int_{-c}^c \mu(z) dz = - \int_{-c}^c \frac{1}{2c} dz = -1, \quad (83)$$

indicating that this focal line image corresponds to the point image of strength -1 that has to be put at the origin in the case of the sphere, as mentioned in Section 1.

Next, working as in the interior case, we conjecture that an image system for the remaining expansion in $N_a^{e, \text{ref}}(\mathbf{r}, \mathbf{r}_s)$ may consist of a point image with strength Q at some interior point $\mathbf{r}_k = (x_k, 0, z_k) = (\xi_k, \eta_k, 0)$, a line image extending from the point \mathbf{r}_k to the focal line along the radial coordinate curve $C : (\eta, \phi) = (\eta_k, 0)$ with density

$$\rho(\mathbf{t}) = \rho(\xi, \eta_k, 0) = \frac{\alpha q(\xi)}{h_{\xi}(\xi, \eta_k)}, \quad (84)$$

where α is some constant and $q(\xi)$ is some continuous function specified in $[1, \xi_k]$, and a surface image on the confocal prolate spheroid $S_{\xi_k} : \xi = \xi_k$ with density

$$d(\mathbf{s}) = d(\xi_k, \eta, \phi) = w_{\xi_k}(\eta) \sum_{n=2}^{\infty} \sum_{m=0}^n d_{mn} C_n^m(\eta, \phi), \quad (85)$$

where d_{mn} are constants to be determined later. Again, the surface image has a total strength of zero and is symmetric with its centroid at the origin. The proposed image system for the exterior Neumann function $N_a^e(\mathbf{r}, \mathbf{r}_s)$ is graphically illustrated in Figure 4.

The potential in the exterior of the spheroid generated by this image system (including the focal line image of uniform density $\mu(z)$) is

$$\begin{aligned} N_a^{e, \text{im}}(\mathbf{r}) &= \frac{Q_0(\xi)}{4\pi c} - \frac{Q}{4\pi |\mathbf{r} - \mathbf{r}_k|} \\ &\quad - \frac{1}{4\pi} \int_C \frac{\rho(\mathbf{t}')}{|\mathbf{r} - \mathbf{t}'|} d\ell(\mathbf{t}') \\ &\quad - \frac{1}{4\pi} \oint_{S_{\xi_k}} \frac{d(\mathbf{s}')}{|\mathbf{r} - \mathbf{s}'|} ds_{\xi_k}(\eta', \phi'), \end{aligned} \quad (86)$$

where $\mathbf{t}' = (\xi', \eta_k, 0)$ and $\mathbf{s}' = (\xi_k, \eta', \phi')$; that is,

$$\begin{aligned} N_a^{e, \text{im}}(\mathbf{r}) &= \frac{Q_0(\xi)}{4\pi c} - \frac{Q}{4\pi |\mathbf{r} - \mathbf{r}_k|} - \frac{\alpha}{4\pi} \int_1^{\xi_k} \frac{q(\xi')}{|\mathbf{r} - \mathbf{t}'|} d\xi' \\ &\quad - \frac{1}{4\pi} \oint_{S_{\xi_k}} \frac{d(\xi_k, \eta', \phi')}{|\mathbf{r} - \mathbf{s}'|} ds_{\xi_k}(\eta', \phi'). \end{aligned} \quad (87)$$

Using (18), we have

$$\begin{aligned} & \frac{Q}{4\pi |\mathbf{r} - \mathbf{r}_k|} \\ &= \frac{Q}{4\pi c} \sum_{n=0}^{\infty} \sum_{m=0}^n H_{mn} P_n^m(\xi_k) P_n^m(\eta_k) Q_n^m(\xi) C_n^m(\eta, \phi), \end{aligned} \quad (88)$$

and

$$\begin{aligned} & \frac{\alpha}{4\pi} \int_1^{\xi_k} \frac{q(\xi')}{|\mathbf{r} - \mathbf{t}'|} d\xi' = \frac{1}{4\pi c} \\ & \cdot \sum_{n=0}^{\infty} \sum_{m=0}^n H_{mn} \left(\alpha \int_1^{\xi_k} q(\xi') P_n^m(\xi') d\xi' \right) P_n^m(\eta_k) \\ & \cdot Q_n^m(\xi) C_n^m(\eta, \phi). \end{aligned} \quad (89)$$

Furthermore, using (18), (85), and the orthogonality relation (13a), (13b), and (13c), we can obtain

$$\begin{aligned} & \frac{1}{4\pi} \oint_{S_{\xi_k}} \frac{d(\xi_k, \eta', \phi')}{|\mathbf{r} - \mathbf{s}'|} ds_{\xi_k}(\eta', \phi') \\ &= \frac{1}{4\pi c} \sum_{n=2}^{\infty} \sum_{m=0}^n H_{mn} \gamma_{mn} d_{mn} P_n^m(\xi_k) Q_n^m(\xi) C_n^m(\eta, \phi). \end{aligned} \quad (90)$$

Demanding $N_a^{e, \text{im}}(\mathbf{r}) = N_a^{e, \text{ref}}(\mathbf{r}, \mathbf{r}_s)$, we have

$$\begin{aligned} & \frac{1}{4\pi c} \sum_{n=0}^{\infty} \sum_{m=0}^n H_{mn} \left[Q P_n^m(\xi_k) \right. \\ & \quad \left. + \alpha \int_1^{\xi_k} q(\xi') P_n^m(\xi') d\xi' \right] P_n^m(\eta_k) Q_n^m(\xi) \end{aligned}$$

$$\begin{aligned}
& \cdot C_n^m(\eta, \phi) + \frac{1}{4\pi c} \sum_{n=2}^{\infty} \sum_{m=0}^n H_{mn} \gamma_{mn} d_{mn} P_n^m(\xi_k) \\
& \cdot Q_n^m(\xi) C_n^m(\eta, \phi) = -\frac{1}{4\pi c} \sum_{n=1}^{\infty} \sum_{m=0}^n H_{mn} \\
& \cdot \frac{P_n^{m'}(\xi_b)}{Q_n^{m'}(\xi_b)} Q_n^m(\xi_s) P_n^m(\eta_s) Q_n^m(\xi) C_n^m(\eta, \phi).
\end{aligned} \tag{91}$$

First, comparing the monopole ($n = 0$) term in both sides of (91), we obtain

$$Q = -\alpha \int_1^{\xi_k} q(\xi') d\xi'. \tag{92}$$

Next, comparing the dipole ($n = 1$) terms in both sides of (91), we get for $m = 0, 1$

$$\alpha g_1^m(\xi_k) P_1^m(\eta_k) = -\frac{P_1^{m'}(\xi_b)}{Q_1^{m'}(\xi_b)} Q_1^m(\xi_s) P_1^m(\eta_s), \tag{93}$$

where

$$g_1^m(\xi_k) = \int_1^{\xi_k} q(\xi') [P_1^m(\xi') - P_1^m(\xi_k)] d\xi', \tag{94}$$

$m = 0, 1.$

Finally, comparing the $n \geq 2$ terms in both sides of (91), we obtain

$$\begin{aligned}
& \gamma_{mn} d_{mn} P_n^m(\xi_k) \\
& = -\frac{P_n^{m'}(\xi_b)}{Q_n^{m'}(\xi_b)} Q_n^m(\xi_s) P_n^m(\eta_s) \\
& - \left[Q P_n^m(\xi_k) + \alpha \int_1^{\xi_k} q(\xi') P_n^m(\xi') d\xi' \right] P_n^m(\eta_k).
\end{aligned} \tag{95}$$

Therefore, the coefficients of the surface image density (85) are given by

$$\begin{aligned}
d_{mn} & = \frac{-1}{\gamma_{mn} P_n^m(\xi_k)} \left\{ \frac{P_n^{m'}(\xi_b)}{Q_n^{m'}(\xi_b)} Q_n^m(\xi_s) P_n^m(\eta_s) \right. \\
& + \left[Q P_n^m(\xi_k) + \alpha \int_1^{\xi_k} q(\xi') P_n^m(\xi') d\xi' \right] \\
& \cdot P_n^m(\eta_k) \left. \right\}.
\end{aligned} \tag{96}$$

To finalize the image system, we have essentially now three unknown values plus one unknown function to decide: Q , ξ_k , η_k , and $q(\xi)$ as a continuous function in $[1, \xi_k]$. They are intercorrelated through the underdetermined system of (92) and (93), so there could be infinitely many different solutions, each giving us a different image system. Below we consider an approach that is again similar to that proposed by Dassios and

Sten in [12]; namely, we choose the unknown function $q(\xi)$ and then determine the other three unknown values. Since, in this case, only proper integrals on $[1, \xi_k]$ are involved, any continuous function $q(\xi)$ on $[1, \xi_k]$ can guarantee the existence of all integrals in (91). For instance, we can simply choose

$$q(\xi) \equiv 1, \quad \xi \in [1, \xi_b]. \tag{97}$$

In this case, by (92), we immediately have

$$Q = \alpha(1 - \xi_k). \tag{98}$$

On the other hand, (93) can be rewritten as

$$x_k = -\frac{P_1^1(\xi_k) Q_1^1(\xi_s) P_1^{1'}(\xi_b)}{\alpha g_1^1(\xi_k) P_1^1(\xi_s) Q_1^{1'}(\xi_b)} x_s, \tag{99a}$$

$$z_k = -\frac{P_1(\xi_k) Q_1(\xi_s) P_1'(\xi_b)}{\alpha g_1(\xi_k) P_1(\xi_s) Q_1'(\xi_b)} z_s, \tag{99b}$$

where

$$\begin{aligned}
g_1(\xi_k) & = \xi_k - \frac{\xi_k^2}{2} - \frac{1}{2}, \\
g_1^1(\xi_k) & = \sqrt{\xi_k^2 - 1} - \frac{\xi_k \sqrt{\xi_k^2 - 1}}{2} \\
& - \frac{\ln(\sqrt{\xi_k^2 - 1} + \xi_k)}{2}.
\end{aligned} \tag{100}$$

Since the point image Q lies on the confocal prolate spheroid S_{ξ_k} , we obtain

$$\begin{aligned}
& \frac{x_s^2}{c^2(\xi_k^2 - 1)} \frac{P_1^1(\xi_k)^2}{\alpha^2 g_1^1(\xi_k)^2} \frac{Q_1^1(\xi_s)^2}{P_1^1(\xi_s)^2} \frac{P_1^{1'}(\xi_b)^2}{Q_1^{1'}(\xi_b)^2} \\
& + \frac{z_s^2}{c^2 \xi_k^2} \frac{P_1(\xi_k)^2}{\alpha^2 g_1(\xi_k)^2} \frac{Q_1(\xi_s)^2}{P_1(\xi_s)^2} \frac{P_1'(\xi_b)^2}{Q_1'(\xi_b)^2} = 1,
\end{aligned} \tag{101}$$

which can be rewritten as

$$\begin{aligned}
& \frac{x_s^2}{a^2} \frac{P_1^1(\xi_b)^2}{\alpha^2 g_1^1(\xi_k)^2} \frac{Q_1^1(\xi_s)^2}{P_1^1(\xi_s)^2} \frac{P_1^{1'}(\xi_b)^2}{Q_1^{1'}(\xi_b)^2} \\
& + \frac{z_s^2}{b^2} \frac{P_1(\xi_b)^2}{\alpha^2 g_1(\xi_k)^2} \frac{Q_1(\xi_s)^2}{P_1(\xi_s)^2} \frac{P_1'(\xi_b)^2}{Q_1'(\xi_b)^2} = 1.
\end{aligned} \tag{102}$$

Equation (102) is a nonlinear algebraic equation for the radial coordinate ξ_k of the point image Q . Unfortunately, this equation does not necessarily have a solution in $(1, \xi_b)$. However, if we choose the constant α as one satisfying

$$\begin{aligned}
\alpha^2 & = \beta^2 \left[\frac{x_s^2 P_1^1(\xi_b)^2}{a^2} \frac{Q_1^1(\xi_s)^2}{g_1^1(\xi_b)^2} \frac{P_1^{1'}(\xi_b)^2}{P_1^1(\xi_s)^2 Q_1^{1'}(\xi_b)^2} \right. \\
& \left. + \frac{z_s^2}{b^2} \frac{P_1(\xi_b)^2}{g_1(\xi_b)^2} \frac{Q_1(\xi_s)^2}{P_1(\xi_s)^2} \frac{P_1'(\xi_b)^2}{Q_1'(\xi_b)^2} \right],
\end{aligned} \tag{103}$$

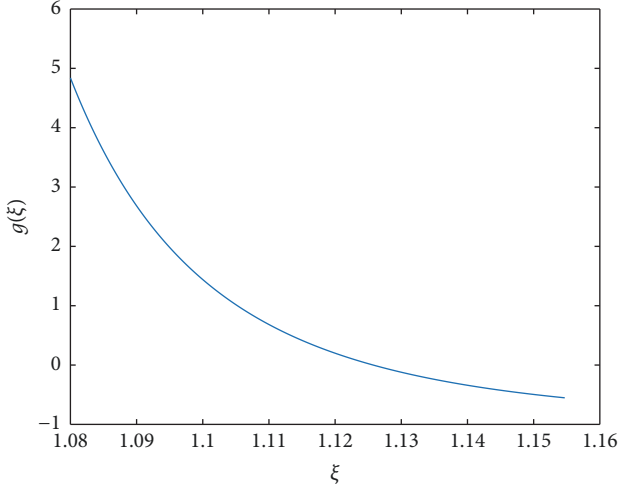


FIGURE 5: The graph of $g(\xi)$ for the case of $a = 1$, $b = 2$, and $\mathbf{r}_s = (1, 0, 2)$.

where β is a constant such that $\beta^2 > 1$, then (102) has a solution in $(1, \xi_b)$. Indeed, define an auxiliary function $g(\xi) : (1, \xi_b) \rightarrow \mathbb{R}$ as

$$g(\xi) = \frac{x_s^2 P_1^1(\xi_b)^2 Q_1^1(\xi_s)^2 P_1^{1'}(\xi_b)^2}{a^2 \alpha^2 g_1^1(\xi)^2 P_1^1(\xi_s)^2 Q_1^{1'}(\xi_b)^2} + \frac{z_s^2 P_1(\xi_b)^2 Q_1(\xi_s)^2 P_1'(\xi_b)^2}{b^2 \alpha^2 g_1(\xi)^2 P_1(\xi_s)^2 Q_1'(\xi_b)^2} - 1. \quad (104)$$

First of all, $g(\xi)$ is continuous on $(1, \xi_b)$. Indeed, when $q(\xi) \equiv 1$, it is easy to see from (94) that both $g_1(\xi)$ and $g_1^1(\xi)$ are continuous on $1 < \xi < \xi_b$ and that $g_1(\xi) < 0$ and $g_1^1(\xi) < 0$ for $1 < \xi < \xi_b$ since $P_n^m(x)$ is strictly increasing on $(1, +\infty)$ for all $n \geq 1$. Then, note that, for $m = 0, 1$, as $\xi \rightarrow 1^+$, we have $g_1^m(\xi) \rightarrow 0$ and thus $g(\xi) \rightarrow +\infty$. Next, it is easy to see that $g(\xi_b) = 1/\beta^2 - 1 < 0$. Therefore, (102) must have a solution in $(1, \xi_b)$. In addition, we note again that the constant β should be chosen in such a way so as to guarantee that the point image is close to the boundary if the source is close to the boundary. For example, we can choose $\beta = (\xi_s/\xi_b)^n$ or $\beta = (Q_0(\xi_b)/Q_0(\xi_s))^n$ for some constant $n > 0$.

We were unable to prove the uniqueness of such a solution, but numerical investigations have suggested that (102) has a unique solution in $(1, \xi_b)$. Figure 5 shows the graph of $g(\xi)$ for the case of $a = 1$, $b = 2$ (so $\xi_b = 2/\sqrt{3}$), and $\mathbf{r}_s = (1, 0, 2)$ with $\beta = Q_0(\xi_b)/Q_0(\xi_s)$. In this case, the unique solution is about 1.12575182. Once ξ_k is found, we can use (99a) and (99b) to calculate x_k and z_k and consequently η_k , and we can use (92) to calculate the strength Q of the point image, respectively.

5. Conclusions

In the present work, we present Neumann functions for the Laplace operator in the case where the fundamental domain is either the interior or the exterior of a prolate spheroid. Three

Neumann boundary conditions are considered, that is, the homogeneous, constant, and nonconstant inhomogeneous boundary conditions. Then, we give image systems for such Neumann functions. For the interior Neumann functions, an image system is developed to consist of a point image, a line image extending from the point image to infinity along the radial coordinate curve, and a symmetric surface image on the confocal prolate spheroid that passes through the point image. On the other hand, for the exterior Neumann functions, an image system is developed to consist of a point image, a focal line image of uniform density, another line image extending from the point image to the focal line along the radial coordinate curve, and also a symmetric surface image on the confocal prolate spheroid that passes through the point image.

Conflicts of Interest

The authors declare that there are no conflicts of interest regarding the publication of this paper.

Acknowledgments

The authors would like to acknowledge the support of the National Natural Science Foundation of China (Grant no. 11471281) for the work reported in this paper.

References

- [1] W. R. Smythe, *Static and Dynamic Electricity*, Hemisphere, New York, NY, USA, 3rd edition, 1989.
- [2] N. S. Koshlyakov, E. B. Gliner, and M. M. Smirnov, *Differential Equations of Mathematical Physics*, North-Holland, Amsterdam, 1964.
- [3] I. V. Lindell, "Electrostatic image theory for the dielectric sphere," *Radio Science*, vol. 27, no. 1, pp. 1–8, 1992.
- [4] W. T. Norris, "Charge images in a dielectric sphere," *IEEE Proceedings Science, Measurement and Technology*, vol. 142, no. 2, pp. 142–150, 1995.
- [5] S. Deng, W. Cai, and D. Jacobs, "A comparable study of image approximations to the reaction field," *Computer Physics Communications*, vol. 177, no. 9, pp. 689–699, 2007.
- [6] I. V. Lindell, G. Dassios, and K. I. Nikoskinen, "Electrostatic image theory for the conducting prolate spheroid," *Journal of Physics D: Applied Physics*, vol. 34, no. 15, pp. 2302–2307, 2001.
- [7] I. V. Lindell and K. I. Nikoskinen, "Electrostatic image theory for the dielectric prolate spheroid," *Journal of Electromagnetic Waves and Applications*, vol. 15, no. 8, pp. 1075–1096, 2001.
- [8] G. Dassios and J. C. Sten, "The image system and Green's function for the ellipsoid," in *Imaging Microstructures: Mathematical and Computational Challenges*, H. Ammari and H. Kang, Eds., vol. 494 of *Contemp. Math.*, pp. 185–195, Amer. Math. Soc., Providence, RI, USA, 2009.
- [9] G. Dassios, "Directional dependent Green's function and Kelvin images," *Archive of Applied Mechanics*, vol. 82, no. 10–11, pp. 1325–1335, 2012.
- [10] G. Dassios, *Ellipsoidal Harmonics, Encyclopedia of Mathematics and its Applications*, Cambridge University Press, 2012.

- [11] C. Xue and S. Deng, “Green’s function and image system for the Laplace operator in the prolate spheroidal geometry,” *AIP Advances*, vol. 7, no. 1, Article ID 015024, 2017.
- [12] G. Dassios and J. C. Sten, “On the Neumann function and the method of images in spherical and ellipsoidal geometry,” *Mathematical Methods in the Applied Sciences*, vol. 35, no. 4, pp. 482–496, 2012.
- [13] C. Xue and S. Deng, “Comment on “On the Neumann function and the method of images in spherical and ellipsoidal geometry”,” *Mathematical Methods in the Applied Sciences*, vol. 40, no. 18, pp. 6832–6835, 2017.
- [14] E. W. Hobson, *The Theory of Spherical and Ellipsoidal Harmonics*, Cambridge University Press, Cambridge, England, 1931.
- [15] P. M. Morse and H. Feshbach, *Methods of Theoretical Physics*, McGraw-Hill, New York, NY, USA, 1953.
- [16] J. Franklin, *Green’s functions for neumann boundary conditions*, 2012, <https://arxiv.org/pdf/1201.6059.pdf>.
- [17] P. Weiss, “On hydrodynamical images. Arbitrary irrotational flow disturbed by a sphere,” *Mathematical Proceedings of the Cambridge Philosophical Society*, vol. 40, no. 3, pp. 259–261, 1944.
- [18] P. Weiss, “Applications of Kelvin’s transformation in electricity, magnetism and hydrodynamics,” *Philosophical Magazine*, vol. 38, pp. 200–214, 1947.



Hindawi

Submit your manuscripts at
www.hindawi.com

